Updating the modern techniques of radiative heat transfer calculation within fuel furnaces and boilers

BORIS SOROKA,
VLADIMIR ZGURSKYI
The Gas Institute of National Academy of Sciences of Ukraine
39, Degtjarivska str., 03113, Kiev
UKRAINE
boris.soroka@gmail.com http://www.ingas.org.ua/index.files/Page14029.htm

Abstract: - Various methods of radiative heat transfer calculations are tested, verified and compared for some applied examples concerning the thermal processes within the working space of boilers and furnaces: of discrete ordinates (DOM) differential approach, of multiple reflections, of similarity with the models of computer graphics, zone method, CFD modeling, stochastic tests with Monte Carlo (MC) procedures. The opportunities and accuracy of MC calculations have been estimated for combustion chambers in 0 (zero), 1-, 2- and 3D statement.

The appropriate radiation models for combustion products have been considered with special attention paid to the model of emissivity of selective (non-grey) gases computed as weighted sum of grey gases (WSGG) mostly compatible with the MC approach.

Due provision the detailed and accurate information on temperature profiles within the volume zones both the thermal state and pollutants formation (particularly of NO) within the combustion chambers could be predicted being fairly coincided with measured data.

Key-Words: - boiler, combustion chamber, environmental pollution, industrial furnace, model of emissivity (absorptivity), Monte-Carlo (MC) technique, NO_x formation, radiative heat transfer, weighted sum of grey gases (WSGG) modelб ray (beam) trajectory.

1 Introduction

Radiative heat transfer makes the principal constituent by performing the calculations of heat exchange processes within combustion chambers.

The radiation process highly exceeds the convection transfer by intensity for high temperature furnaces however the complicated heat transfer: by radiation and by convection - should be considered in combination to satisfy the accuracy requirements relevant to development new designs of combustion chambers or for optimization the operation modes of the power boilers and industrial furnaces.

The chosen calculation method and proper procedures should be admissible to perform the solution both the direct and inverse tasks of heat exchange in the furnaces and boilers.

By direct statement the task the temperature profiles, pattern of optic characteristics of media along with the heat sources, heat sinks and receivers arrangement within the furnace space is necessary to set preliminary. Flows vectors within the chamber should be taken into consideration side by side with thermal physical properties of the moving media and those for the surrounding surfaces. Definition of the local heat fluxes and total absorbed heat reception could be provided by these conditions both through selective (for given wavelength λ) constituents and integral emissivity (on the whole and first of all – in infrared range of λ) ones. Inverse or mixed problem solution requires the temperature pattern recovery to predict the thermal state of the combustion or furnace chamber within the furnace or its part.

Usually the integration, averaging and smoothing procedures are changed for discrete operations because of complications with the theoretical (functional, differential) presentation of each from above mentioned characteristics and properties within the chamber, first of all regarding gas emissivity/absortivity distribution by coordinates (by space) and that on radiation intensity change from point to point of studied space.

The Monte Carlo (MC) procedure provides definition of generalized and detailed characteristics of the system under consideration being in statistical response on the local perturbation issued from the points inside the system. The MC procedure in combination with proper techniques or even independently assumes consequent consideration of interaction of the discrete energy beams with each of zones (volume and surface).

Various existing MC procedures including those purposed for non-steady state calculations (for example [1]) are differed by law of option the consequence of mentioned procedures, on the technique of space division by zones, are distinguished by type of MC randomizer and by technique of stochastic (random) searching of the computation nodes, with radiation beams tracking, and by selection the most suitable emissivity model (see below). Finally the MC techniques are varied by accuracy of computations. The following sections are discussed below:

- The existing modeling opportunities of prediction the thermal state of combustion plant.
- The proposed MC technique and its place by calculation the radiative and complicated heat transfer process and facilities.
- Some examples of validation and application the proposed MC technique by estimation the thermal state of the furnaces and boilers.
- Application the MC procedures to evaluate the environmental characteristics of the combustion processes and plants.

2 Calculation the radiative and complicated heat transfer: modern techniques

2.1. Zone method

Both design and checking types of the boilers' and the industrial furnaces' calculations are suitable to perform by means of the zone method of heat exchange computation.

This method consists in determination of the temperature profiles within the gas volumes and at the fence surfaces of the furnace along with computation of the resulting heat fluxes – at the receiving surfaces of the charge to be preheated or of preheating the hot water tube sections.

The method is performed as follows [2]:

- by means of H. Hottel's (USA) statement of determination of areas of radiative energy exchange: direct, total, directed;

- by means of the statement by Ju. A. Surinov and his followers (former USSR), including the scientific schools of the Moscow Institute of Steel and Alloys (B.S. Mastryukov, V.A. Arutyunov) and of Ural Polytechnic Institute (V.G. Lisienko) by means of determination of the angle factors: ordinary, generalized, resolving.

To use the zone method it's necessary to assign in advance the pattern of the flue gases flow within the furnace space, as well as to obtain the preliminary information on fuel burning and heat release processes.

Afterwards the furnace under consideration would be divided by the computation zones. The heat balance equations for each of the zones are to be concluded. The resulting fluxes within the balance equations would determined by both of them, transferred by radiation and convection with account of the heat fluxes emitted by the current zone under consideration particularly in form of effective radiation of the surface emitting zone.

2.2. Computational Fluid Dynamics (CFD - code)

Approach under consideration is conformable both for design and checking types of heat calculation of the furnaces. Heat calculation of the boiler by using of CFD procedures presumes the simultaneous determination of the local temperature pattern within the gas volumes and at the adiabatic setting surfaces (or those approximate to the last ones with account of the heat losses) as well as the calculation of the heat fluxes profiles absorbed by the receiving surfaces – by the furnace ingots or by the water cooled tube sections.

Application of CFD-modeling by means of well-known computer codes of ANSYS' products for Fluid Dynamics computation (including dozens versions of Fluent codes, CFX, CFD-Flo) or more simple PHOENICS one allows to search for the local characteristics of the furnaces, but, unfortunately, it is characterized by complexity of statement of the limiting and boundary conditions [3-5]. We have to say in addition that the basic elements of CFD-models are the blocks of computation of momentum, energy and mass transfer [3,5] with account of the models of turbulence and (for exchange the k-ε one) as well as the models of combustion by two various approaches: by assumption of thermodynamic equilibrium of heat carrier flow (Fast Chemistry Approach (FaCA)) or by account of limiting effect of the combustion kinetics (Finite Chemistry Approach (FiCA)) [6-9].

In the first case (FaCA), the main attention has been paid to simultaneous simulation of the processes of turbulent mixing and combustion. The calculation is being performed through limiting component of combustion ("excess fuel" - mixture fraction) [7,9,10] by means of numerical empirical factors. Stochastic behavior of turbulence is taken into account by the probability distribution function (PDF – probability density function) [7].

Such modern combined models of turbulent combustion – mixing without detailed elaboration of kinetics, but with the capability of calculation of the progress of flame process, were begun by D.B. Spalding (Eddy Break Up (EBU) - model) [6], and developed afterwards by B.F. Magnussen: Eddy Dissipation Model (EDM), Eddy Dissipation Concept (EDC) and their followers: Flame Sheet Model (FSM), Laminar Flamelet Model [8, 11], including the program "RUN-1DL Code" [11]).

The source member of the energy equation represents the divergence of a radiant flux vector when this vector is surpassing other ones by heat transfer calculations. Intensity of radiation is determined by using the radiant transfer equation (RTE). This equation is solved by means of S_4-approximation of the discontinuous ordinate method has been elaborated by J.S. Truelove [7] with account of the directions of the energy radiation and alteration of intensity along the beam trajectories.

As to computation of radiative transfer within the framework of particular codes (FLUENT, for example), 6-beams DTRM method (Discrete Transfer Radiation Model) [12] is used. This method that is also referred as 6-flux approximation of the radiative transfer equation, takes into account directions of anyone of calculated direct and return beams [5].

The discrete ordinates (DO) radiation model (DOM) solves the radiative transfer equation (RTE) for a finite number of discrete solid (spatial) angles, each associated with a vector direction $\vec{s}$ fixed in the global Cartesian system (x, y, z) [13]. The fineness of the angular discretization being under consideration is analogous to choosing the number of rays for the DTRM (discrete transfer radiative model). Unlike the DTRM, the DO model does not perform ray tracing by consideration the radiation transport equation for intensity in the spatial coordinates (x, y, z). The DOM approach solves for as many transport equations as there are directions $\vec{s}$. So S_6 approximation could be assumed as one of the recommended techniques for particular implementation.

Like DOM the "Ray tracing" method is applied by engineering techniques with S_n quadratures based on selection of n transfer directions. In this case by operation with n constituents each of them are to be taken with own weight factor. Particularly in example given in [14] only 4 (four) shares was used to satisfy an account of spatial pattern of radiative energy, that means $S_n = S_4$.

2.3. Method of stochastic tests

In frame of both: zone and CFD-methods, the Monte-Carlo (MC) procedure could be used to compute the angle coefficient (view factors) of radiative exchange. The method's substance consists in calculation of the energy portion absorbed by the zones (both volume and surface ones) by mutual radiation exchange between the zones. The procedure is performed by means of application of the random number generator by determination of the coordinates of emittance sources and directions of the energy fluxes emission in accordance with the mentioned numbers.

At each stage of radiative heat exchange calculations the direct Monte-Carlo procedure is performed. The temperature profiles are assigned in advance independently on type of task to be solved: direct or inverse. The resulting heat fluxes profiles along the receiving surfaces within the furnace space grounded on these profiles are under consideration. The procedure provides to predict non-uniformity of the local heat fluxes (incident, absorbed, resulting) patterns within the volume and surface zones and in dependence on the optic characteristics of the media. The relevant characteristics would be given in advance as well.

2.4. Method basing upon similarity of propagation the emissivity of various wavelengths

2.4.1. Processes of heat transfer by radiation in infrared range of wavelengths and of visible light propagation laws are similar, since mentioned phenomena are distinguished only by specific fractions of spectrum where each of other processes takes place. For range of wavelengths for visible light such phenomena as diffraction and interference could be significant while, at the same time for calculation the heat transfer processes these phenomena have no significant influence.

This similarity is of practical importance. Thus, the similarity and difference in approaches and methods of calculation the radiative heat transfer and the computer graphics solutions are discussed in detail in [15]. Table 1 presents the comparison [15] of main characteristics of *Domke's* analysis of computer graphics and of radiative heat transfer to be studied for different tasks.

In our work we will try to use the advantages of the algorithm of 3D computer graphics by means of using the homogenous coordinate system (see below).

Table 1. Main features of the computer graphics model and radiative heat exchange model (accordingly [15])

Model of computer graphics	**Model of radiative heat exchange**
Phenomenon analysed	
Propagation of electromagnetic waves in visible radiation range $\lambda \in$ (0.380 - 0.780) μm	Propagation of electromagnetic waves in infrared radiation range $\lambda \in$ (0.780 - 1000) μm
Final goal of modelling	
Photorealistic image of the observed scene	Distribution of the temperatures and heat fluxes by the surfaces
Required intermediate stage	
Distribution of illuminance on observed surfaces	Distribution of absorbed heat fluxes by analysed surfaces
Essential primary phenomena	
Generation and propagation of radiation	Generation and propagation of radiation
Diffusive reflection, specular reflection	Diffusive reflection, absorption
Secondary phenomena taken into account	
Direct reflection, diffraction, polychromatics	Specular or direct reflection

Analysing the basic equations of computer graphics and of radiative heat exchange becomes evident that both are nearly identical. It follows from the fact that they describe the same phenomenon, i.e. generation and reflection of the electromagnetic waves in arbitrary or accidental directions. Computer graphics procedures and models make the subset of radiative heat exchange procedures and models, as in solving tasks related to the lighting technology one can adopt much more far-reaching simplifications than by radiative exchange [15]. However, the computer graphics technologies with new improved computational procedures and simulation models have been grown in recent years much more stronger and rapidly than conservative scientific branch – heat transfer by radiation. The possibility of using the existing tools in form of computer graphics software to compute radiative heat transfer makes the separate research task and is of great practical significance.

Radiative heat exchange is described in the notions of thermal values (temperature, radiative heat flux or power density) while for computer graphics application the defining effect makes luminous flux (luminosity). An adjustment of computer graphics programmes for modelling and numerical simulation the radiative heat transfer requires mutual conversion the thermal values and luminosity with account of boundary conditions describing radiative heat transfer systems.

The impressive state of photorealism at the images received and created by application of the techniques of the modern computer graphics was stipulated by fast advancement of the computer technologies and of appropriate development of relevant software. By modern computers application the plurality of three-dimensional objects could be rendered with high productivity, often in real time. Required procedure is performed by means of application the special optimized algorithms and custom commands of the instruction central processor and of the graphics system (CPU and GPU – respectively) being optimized for rendering the 3D models.

2.4.2. The modification of the technique being known in 3–dimensional computer graphics was proposed to use for generalization the procedure. This approach consists in the compact description of the geometrical conversions by means of uniform coordinates' method. The last is applied in the OpenGL and DirectX codes [16, 17]. General arrangement of the objects within the area under consideration is suitable to present in global world system of coordinates, while the beams transformation – in the local system connected with the point of emittance or absorption, intersection of the beam with the object – in the system connected with the certain object. As a result the approach is required enabling to perform any transformations of coordinate systems. Matrix form presentation ensures optimum performance.

Classic geometric transformation (displacement, turn) consists in some separate conversions of matrixes of size 3×3, each bringing to gather by great massive of computations. To simplify the procedure, new technique has been developed basing upon the method of homogenous (uniform, similar) coordinates. In framework of the method the point in 3-dimensional space is presented by four components $|W{\cdot}x,\ W{\cdot}y,\ W{\cdot}z,\ W|$, where $W\neq 0$. By means of the method of homogenous coordinates the single matrix envelops any transformations, including displacement, turns, projections of various views along with combination of transformations. By our approach we've used W=1 and obtained normalized coordinates (x, y, z, 1).

The process called *matrix concatenation* accounts the matrices transformation. The order in which the matrix multiplication is performed is crucial.

2.5. Gas emissivity models

2.5.1. Accounting of optical characteristics of combustion products including dependences of coefficients of the radiation attenuation (of varying the absorption and of scattering factors) is of the greatest significance by heat transfer calculation within combustion chambers filled in with selective emitting and absorbing medium. Various models of 3-atonic gases emissivity and radiative properties calculation like "statistical narrow band (SNB)", "absorption distribution function (ADF)", "exponential wide-band (EWB)"[14] make constituent of any procedure of calculation the radiative transfer in combination with consideration of dependences of the monochromatic radiative properties on the wavelength with account of opportunity of their averaging.

Generalization of the properties instead of integration by spectrum is performed by means of application the weighted sum of the respective characteristics under consideration within each of i-th fraction of the spectrum wavelengths.

This approach has been used in [14] where the process of combined radiation and laminar forced convection within cylindrical duct has been studied. Mathematical model is composed of the system of differential equations of continuity, movement and energy (mass, momentum and energy balance (conservation)) for stationary flow of axially symmetric superheated water vapor. Value of $div\,\vec{q}_r$ for radiative heat flux makes the source member in the equation of energy where the spectral and spatial components are twice summarizing (integrating) by each of respective variables.

2.5.2. Another important input in change of optical properties of combustion products is connected with account of solid (mainly carbon) particles formation in combustion products.

For example by the engine operation the smoke opacity makes an indirect soot indicator in exhaust gases while the fuel and its burning is involved in the process of suspended powders forming [18].

Variation of absorption factor (coefficient) for non-transparent medium in dependence on composition of the gases, on particles content and of their number is similar by impact to corresponding relationship for opacity of flue gases [18].

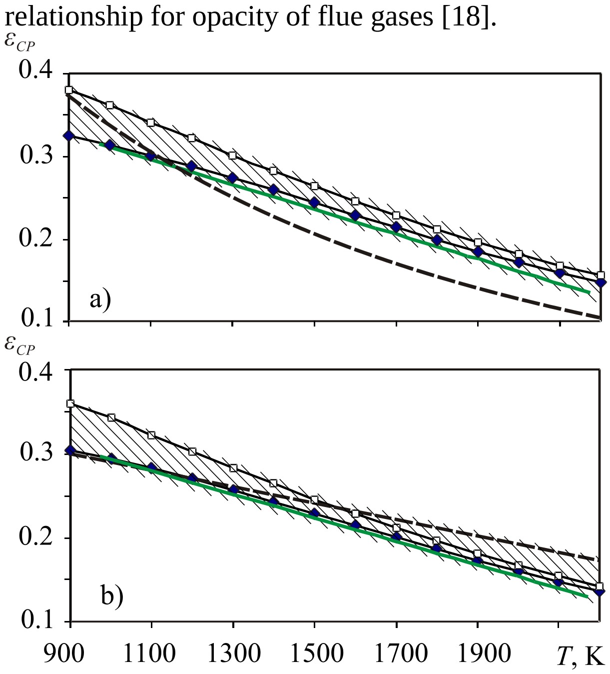

Fig. 1. Integral emissivity (blackness) factor of the combustion products ε_{CP} been calculated by means of various models.
a – coke-oven gas as a fuel (p_{H_2O} = 0.239, p_{CO_2} = 0.07, Δl=1m); b – natural gas as a fuel (p_{H_2O} = 0.190, p_{CO_2} = 0.095, Δl =1m).

- in accordance with B. Leckner's model [24];
- by means of narrow band model [25];
- by means of WSGG model [19,22,23];
- by means of H. Hottel's charts for CO_2 and H_2O [22, 25].

It was stated under very high resolution that spectra of low resolution are composed of a number of lines over which the true spectral absortivity varies greatly [19]. For the fossil fuels the monochromatic radiation transmissivity τ_λ of the flat layer of thickness Δl or Δl_{ef} – effective thickness of layer filled in with mixture of CO_2 – H_2O – soot containing combustion products could be given by equation:

$$\tau_\lambda = \exp(-k_{\lambda,CO_2} p_{CO_2} - k_{\lambda,H_2O} p_{H_2O} - k_{\lambda,S} c_S)\,\Delta l \qquad (1)$$

In equation (1) the following nomenclature was used: k_λ – monochromatic (spectral at wavelength λ) attenuation coefficient, p_{CO_2}, p_{H_2O} – partial pressure of CO_2 and H_2O in gas mixture – respectively; c_S – soot concentration in gas mixture.

2.5.3. Selectivity and non-isothermal state of the gas volume of non-grey gases were taken into account by use of H. Hottel's model [7,8] and by representation of the integral emissivity factor ε_g and absorption abilities A_g of real gas (combustion products) by means of weighted sum of radiation of n grey gases each of them being characterized by absorption factor k_n not depending on temperature. Contribution of the *n-th* gas radiation depends on gas T_g or emitter T_e temperature, the corresponding fraction a_n (weighting factor) being submitted to the condition of normalization:

$$\varepsilon_g = \sum_n a_n\left(T_g\right)\left(1-e^{-k_n p_\Sigma \Delta l_{ef}}\right); \qquad (2)$$

$$A_g = \sum_n a_n\left(T_e\right)\left(1-e^{-k_n p_\Sigma \Delta l_{ef}}\right); \qquad (3)$$

$$\sum_n a_n = 1, \qquad (4)$$

where $p_\Sigma = p_{CO_2} + p_{H_2O}$; $K_n = k_n p_\Sigma$ (5)

Various approximations for non-grey radiation are collected in the literature where the number n makes value between 3 up to 6 components [5] and even up to 19 [20]. The a_n and k_n values for the combustion products of natural gas ($p_{H_2O} = 19$ kPa, $p_{CO_2} = 9.5$ kPa) were taken accordingly Taylor and Foster data [19] by number $n = 4$ in our calculations have been performed earlier and within the framework of the present paper.

We'll call the *n-th* grey gas contribution in case of non-grey gas as *n-th* "quasi-level" by analogy with the structure of the selectively emitting gas. Using Monte-Carlo procedure accordingly [21] the different random numbers must correspond to each of "quasi-levels" of non-grey radiation. This approach simulates subjecting of the selective radiation characteristics to stochastic computation procedures.

Total emissivity of CO_2-H_2O-soot mixtures arising in oil and gas combustion have been computed from the statistical band model and experimental spectral data for the gases and from the optical constants of soot using the Mie theory [19].

Account of presence of the particles in combustion products by application of the model of weighted sum of grey gases (WSGG) for non-grey radiation of emitting and absorbing medium becomes clearly evident due simple summation of radiation's attenuation

$$K_n = k_{g,n}(p_{CO_2} + p_{H_2O}) + k_{s,n} \cdot c_S \qquad (6)$$

by multi- atomic gas components (water vapour and carbon dioxide) and discrete particles or cloud of the particles where $k_{g,n}$ is the specific attenuation (absorption) by gas mixture at n-th quasi-level while $k_{s,n}$ meets absorption and scattering of medium due soot influence on incident radiation.

2.5.4. The Monte–Carlo (MC) procedures [17] been developed by our team is compatible with the weighted sum of grey gases model of the integral emissivity (WSGG) [22]. It has been collected a lot of the WSGG presentations for the combustion products of the natural gas *(NG)*([H_2O] : [CO_2] = 2:1), including well known equation by Taylor and Foster [19]. For combustion products of the coke – oven gas (COG) is known the WSGG equation for the case of [H_2O] : [CO_2] = 3.4 : 1[23].

In Fig.1 are compared the integral emissivity ε_{cp} values versus gas layer temperature T computed by means of the codes developed by our team in accordance with various models: exponential wide band (by B. Leckner) [24], narrow band [25], WSGG [19,23], on the one hand, and accordingly H. Hottel's diagrams for CO_2 and H_2O with account of the bands overlapping [26], on the another hand. The maximum divergence of the ε_{CP} values by various models and the charts doesn't exceed 15…25% – for the *NG* combustion products against 15…35% – for the COG products.

2.6. Authors' development of the Monte Carlo procedure

2.6.1. The proposed MC procedure in rectangular Cartesian and polar coordinates has been developed for the furnaces filled in with combustion products, the last presenting an opaque (or non-transparent) medium [17].

2.6.2. Like the computer graphics approach, computation backgrounds of radiation transfer particularly regarding the Monte-Carlo procedure consist of tracing the space by energy rays (beams) from the emission point (from the source) until disappearance the ray's energy (e.g. absorption).

In practice movement of the beams (rays) is analysed until the energy remainder transmitted with the beam under consideration exceeds the value ξ<1% initially emitted energy.

Key distinction between the processes under consideration makes different description of the light propagation system and that for the thermal system. The ranges of acceptable simplifications one of another are also differed.

2.6.3. To fulfill the numerical procedure, the total energy emitting by each surface or volume zone is divided between N emitting beams. Each of the beams equations is presented in form

$$x = x_0+r_x t,\ \ y = y_0 + r_y t,\ \ z = z_0+r_z t, \tag{7}$$

where x_0, y_0, z_0 – the source coordinates, r_x, r_y, r_z – the guiding (direction) cosines, t – the variable characterizing the distance by beam from the emitting point. Verification of the beam's pathway is carried out for each object to evaluate intersection (the minimum t value meets the first direct hit and reflection). The detailed procedure has been described [17,28] in frame of mathematical MC model [29] of definition the resulting heat fluxes due repeated summation of energy input absorbed in j-th volume zone by following four variables: emitting zones i, number N_i of rays (beams), emitted from zone i, number h of the re-radiation (reflection) cycle, number of n for the n-th quasi-level of the WSGG model (see sub-subsection 2.5.3).

2.6.4. By our present performance the approach is changed as contrasted to the paper [21]: the complete cycles of statistical trials are fulfilled for each of n grey gases in the same manner. The similar procedure was recommended in the manual [30] for separate spectral intervals of selectively radiating gas.

The difference of the method, originated by us, from those in the book [30] makes the strong direct calculation of resulting heat fluxes by radiative transfer between all volume and surface zones while in [30] the spectral resolvent angular (view) coefficients (SRAC) were computed basing upon optical and geometrical performance between volume and surface zones inherent to the enclosure.

By using the H. Hottel's zone method grounded upon WSGG model of radiating gas and surfaces of mutual exchange the total interchange areas represent the values corresponding to SRAC in frame of technique based on complicated view factors (see section 2.1.).

3 Verification of Monte-Carlo technique by prediction the thermal state of the boilers and furnaces

To estimate the adequacy of proposed MC technique and to verify the last by estimation of thermal state of the fuel furnaces and boilers a great deal of processes and combustion plants have been computed with various known methods both for stationary and non-stationary cases.

The non-steady process for moving heat-exchanging media was presented by stationary form within the furnace space for any cross-section.

3.1 Uniform zero-dimensional gases temperature pattern

Validation of developed MC procedures has been carried out in comparison with computation data obtained by H. Kremer for the chambers with the single given uniform temperature [24] at fuel-use plants: boilers and furnaces.

To compare the results of calculations in accordance with the zone and Monte Carlo methods, the Kremer's data [31] were verified relatively our computations. The combustion chambers of the simplest box design were tested by means of modeling of both boiler unit or tube process furnace (Fig.2) and the reheating industrial furnace (Fig.3). The specific and total absorbed heat fluxes have been defined basing upon temperature conditions within the chamber and depending on O_2 content in combustion air.

By comparison of numerical data (Fig. 2 and Fig. 3) it has been concluded that dependences on total heat absorption computed by two various methods are similar and sometimes numerically coincided. But the resulting total heat fluxes (Q_w, Q_M) and the local specific fluxes (heat fluxes density q) in accordance with Kremer's and our calculations are diverged, the discrepancy between computed values being varied in dependence on furnace temperature and on O_2 content in combustion air. Difference between mentioned data makes 10…15% and usually doesn't exceed 20%.

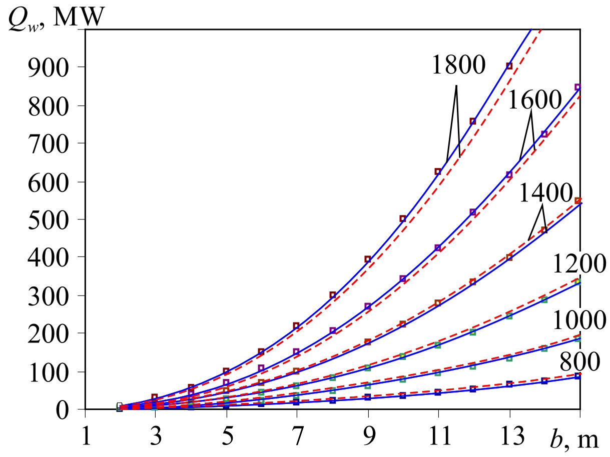

Fig. 2. Total heat flux Q_w absorbed by the receiving surfaces (walls) of the boiler or process furnace in dependence on combustion chamber width *b*.
Solid lines – our calculations by Monte-Carlo procedure, dotted lines – by H. Kremer [31]. Zone method computations parameter – furnace gas temperature T_g, °C, is indicated near the curves. Number of computation zones N_{CZ} =1.
O_2 content in oxidant $[O_2]$ = 100%.

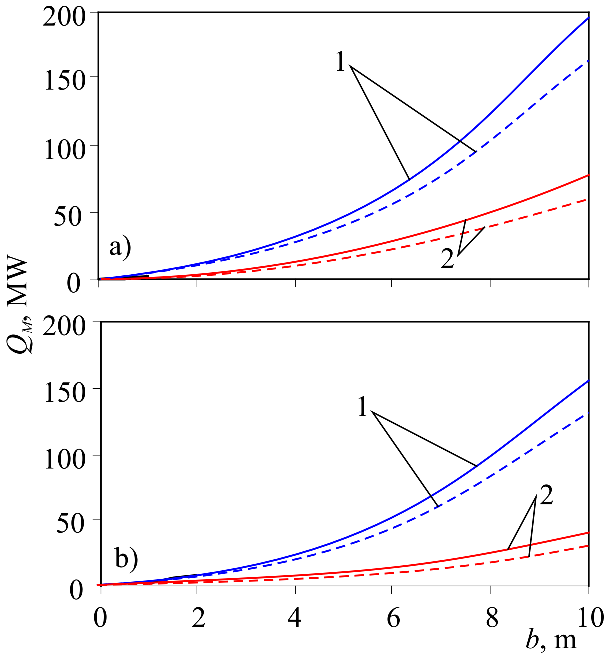

Fig. 3. Resulting total radiative heat flux Q_M, absorbed by ingot surface in the industrial furnace.
Ingot temperature T_M , °C: a – 800; b – 1200.
Furnace gases temperature T_g, °C: 1–1800; 2–1400;
Solid lines – our calculations by Monte-Carlo procedure, dotted lines – by H. Kremer [31].
Number of computation zones N_{CZ} =1.
Zone method computations parameter – furnace gas temperature T_g, °C. $[O_2]$ = 21% in oxidant.

3.2 One-dimensional gas temperature profile within the furnace chamber

3.2.1. The radiative and convective heat transfer process was considered for flat layer of combustion products of one-dimensional temperature profile $T_g(l)$ within the space located between two surfaces. The temperature pattern was uniform by the planes parallel to the planes enclosing the layer.

Thus computation area represents two infinite parallel plates: the radiator (emitter) *K* – an adiabatic brickwork of unknown temperature T_K and the receiver *M* of given temperature T_M – enclosing the flat gas layer of Δl_Σ thickness, the last being filled in of the completely burnt gases-combustion products of natural gas. Two different approaches have been used by calculation the resulting specific heat flux q_M and refractory temperature T_K: multiple reflections procedure and MC procedure.

Table 2. Temperature pattern of the gas layer sections across the gas flat volume within the furnace by various heat transfer conditions: uniform distribution, direct, indirect, direct + indirect heating (in accordance with classification [32]).

Section site #	Direct + indirect	Direct		Indirect				Uniform distribution	
	K / M	K / M	K / M	K / M	K / M	K / M	K / M	K / M	K / M
	1	2	3	4	5	6	7	8	9
1	1700	1300	1300	1700	1700	1600	1570	1400	1300
2	1570	1330	1330	1570	1655	1570	1700	1400	1305
3	1470	1335	1335	1475	1625	1550	1475	1400	1310
4	1380	1340	1340	1445	1595	1530	1445	1400	1315
5	1330	1345	1345	1420	1565	1510	1420	1400	1320
6	1320	1350	1350	1405	1535	1490	1405	1400	1330
7	1315	1355	1355	1395	1505	1470	1395	1400	1380
8	1310	1360	1360	1385	1475	1450	1385	1400	1470
9	1305	1365	1365	1380	1445	1430	1380	1400	1570
10	1300	1370	1370	1375	1415	1410	1375	1400	1700
11	1300	1375	1375	1370	1385	1390	1370	1400	1700
12	1305	1380	1380	1365	1355	1370	1365	1400	1570
13	1310	1385	1385	1360	1325	1350	1360	1400	1470
14	1315	1395	1395	1355	1295	1330	1355	1400	1380
15	1320	1405	1405	1350	1265	1310	1350	1400	1330
16	1330	1420	1420	1345	1235	1290	1345	1400	1320
17	1380	1445	1445	1340	1205	1270	1340	1400	1315
18	1470	1475	1475	1335	1175	1250	1335	1400	1310
19	1570	1570	1700	1330	1145	1230	1330	1400	1300
20	1700	1700	1570	1300	1100	1200	1300	1400	1300

Temperature T_g profiles across the gas layer is submitted in the Table 2. The gas layer is divided upon $N = 20$ equal discrete sections of the same thickness. Numbering of the sections is beginning from the layer ($i = 1$), being the nearest to the refractory wall K. The layer contacting with the receiver wall is numbering as $i = N = 20$. Various temperature profiles were compared from the efficiency standpoint (estimation of the maximum q_M value) [32]. The temperature profiles in Table 2 were assigned in such a manner that an averaged temperature value was conserved for any of nine variants being under consideration:

$$\overline{T}_g = \frac{1}{\Delta l_\Sigma} \int\limits_{(\Delta l_\Sigma)} T_g dl = 1400\,K = idem \qquad (8)$$

It was supposed, that the resulting heat flux being absorbed by enclosing surfaces $S \in \{M, K\}$ includes radiative q^S_{rad} and convective q^S_{conv} components in frame of additivity ability:

$$q_S = q^S_{rad} + q^S_{conv}\,;\ q_K = 0. \qquad (9)$$

The convective heat fluxes to each of enclosing surfaces were computed from the standpoint for coefficients of convective heat transfer α_{conv}

$$\alpha^M_{conv} = \alpha^K_{conv} = const = 23.2\ \mathrm{W/(m^2{\cdot}K)} \qquad (10)$$

The surfaces M and K, enclosing the gas layer, were assumed as grey bodies by performance of calculation.

Numerical computations with MC procedures (Fig.4,a) were carried out by means of substitution the infinite flat layer for volume structure of finite sizes one surrounded by specular reflection side surfaces. In Fig.4,b are presented the resulting heat flux values being calculated by means of multiple reflections technique in frame of WSGG model of gas emissivity [32]. Thus comparison of the resulting heat fluxes q_M for various temperature profiles across the layer gives fairly coincided data for two computation procedures under consideration (Fig.4, a,b).

3.2.2. The situation connected with influence the temperature profile across the gas (combustion products) layer becomes ambiguous for the case of appearance the discrete particles within the gas medium. We've considered the same by geometry layer of combustion products corresponding to layouts of Table 2 when the oil was used as a fuel instead of natural gas. The same temperature profiles of nine forms those were analyzed in direct statement by resulting heat transfer (heat flux) intensity q_M were calculated by multiple reflections procedure while the liquid fuel is burning in the studied system.

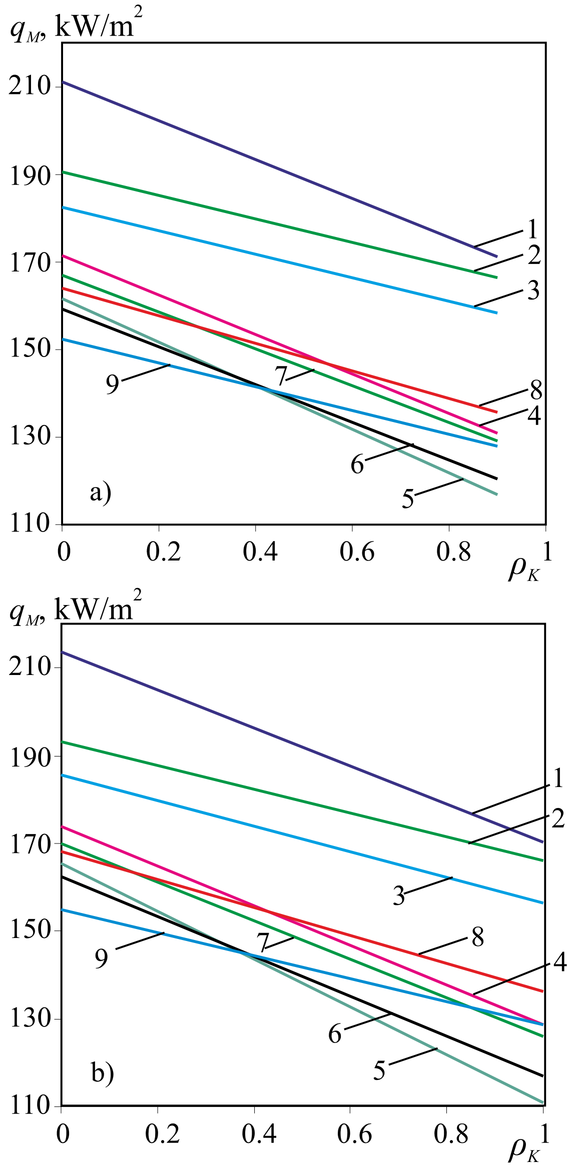

Fig.4. Dependence of resulting heat flux density q_M absorbed by receiving surface of flat layer of natural gas combustion products in dependence on reflectivity of adiabatic refractory surface ρ_K.

The number of the curve corresponds to the variant of temperature pattern across the flat layer of natural gas' combustion products (Table 2):

a – our calculations by Monte-Carlo procedure. Relative energy remainder $\xi = 0.002$;

b – our data being computed by multiple reflections procedure and adopted from [32].

The generalizing data on comparison the heat transfer intensity under natural gas (*NG*) and liquid fuel (*l*) combustion are summarized in Fig.5. The following ratios have been chosen as the characteristic values by evaluation the opportunities of radiative heat exchange for gas and liquid fuels' combustion products:

$$\begin{cases} \overline{q}_M = q^l_{M,j} \,/\, q^{NG}_M; \\ \overline{q}_{M,j} = q^l_{M,j} \,/\, q^{NG}_{M,j}; \\ \overline{q}_{M8} = q^l_{M,j} \,/\, q^{NG}_{M,8}. \end{cases} \qquad (11)$$

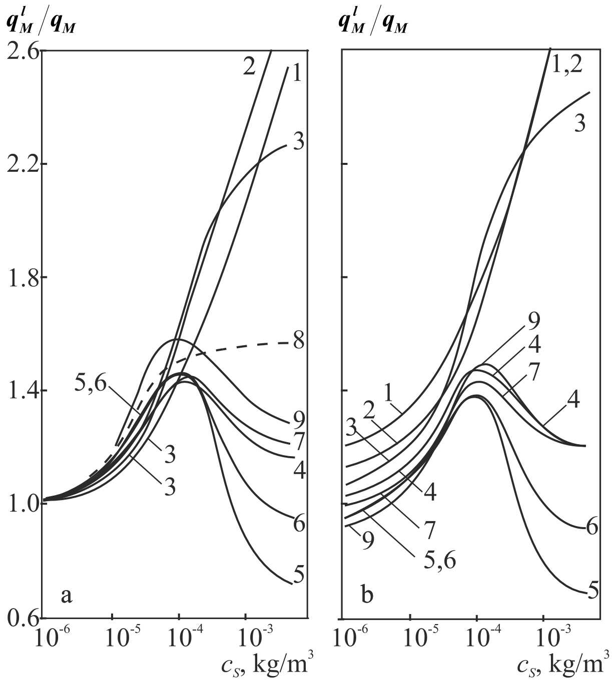

Fig.5. Relative value $\overline{q}_{M,j}$ of specific resulting heat flux absorbed by receiver under liquid fuel combustion to that obtained by natural gas burning in dependence on soot concentration c_s (kg/m^3) in combustion products.

a – for $\overline{q}_{M,j}$ value compared to $q^{NG}_{M,j}$ under *NG* combustion related to *j*-th (j = 1 – 9) temperature profile within the layer.

b – for $\overline{q}_{M,j8}$ compared to heat flux under uniform temperature profile within the layer of *NG* combustion products (j = 8).

The numbers near the curves correspond to temperature profiles (Table 2).

T_G = 1400 K, T_M = 300 K, $\varepsilon_M = \varepsilon_K$ = 0.8.

In Fig.5,a through the value $\overline{q}_{M,j}$ are compared the respective fluxes for the *j*-th variant of temperature profile. In Fig.5,b the most advantageous temperature profile by oil combustion under given c_s could be estimated due comparison with value q^{NG}_{M8} = const = $f(c_s)$. This approach is suitable to make option from the maximum resulting heat flux standpoint.

If maximum temperature by layer is located near heat absorbing surface M the resulting heat flux q_M is growing with soot concentration rise. In case of uniform temperature profile the $q^l_{M,8}$ value becomes asymptotic to maximum value by $c_s \sim 10^{-4}$ kg/m^3. In any other case (profiles j = 4,5,6,7,9) the optimum c_s values exist providing maximum resulting heat fluxes $q_{M,j}$ corresponding to layer of chosen temperature profile and to given c_s value.

3.2.3 In case of more complicated – stepped temperature profile by furnace height – comparison with zone method has been carried out for the tube furnace. Temperature was uniform in the planes parallel to furnace bottom across the gas heating medium flow.

Thermal calculations have been performed by means of Monte-Carlo (MC) procedure to account radiative heat transfer constituents while neglecting convective ones. The task has been solved in fundamental statement by assign in advance of the gas temperature profiles within the furnace space by height (Fig. 6).

The boilers' furnaces geometry of traditional hot - water and steam types of middle thermal capacity could be presented mainly as the parallelepiped of the sides dimension of $b \times b \times 2{\cdot}b$ or at least $b \times b \times 1.5{\cdot}b$.

The process (cracking) furnace accordingly E. Scholand [33] (Fig. 6,a) doesn't differ from standard boilers geometry in essence and is similar to TVG–8 boiler by design: furnace is supplied with hearth (bottom) type burners and by plants operation the vertical flames are developed upwards, parallel to the heat reception water tube walls.

The water tube boiler for comparison with the furnace (Fig. 6,a) is TVG-8 design (Fig. 7,a). This type of boilers is distinguished by furnace space partitioning: for 4 sections (by means of arrangement of 3 two-side water tube screens).

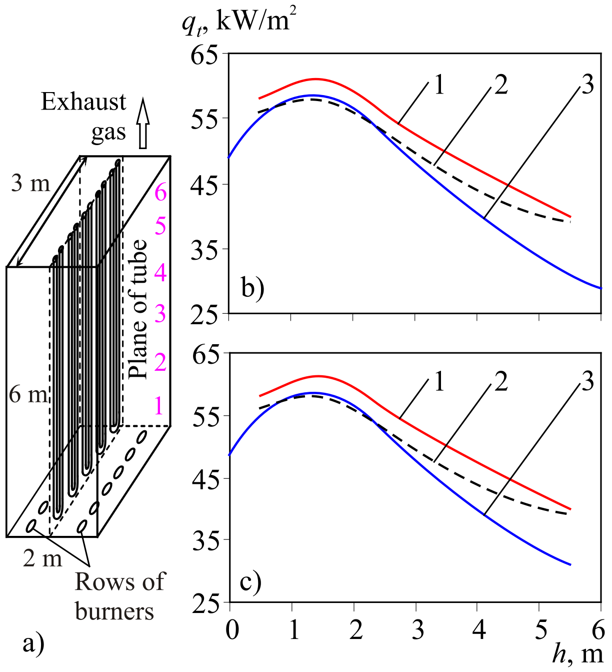

Fig. 6. Profile of resulting heat flux density q_t by furnace height h / Comparison of our original predicted data with earlier calculations.

a – cracking furnace. Number of computation zones/ zone sizes (m^3): b – 6 / 1×1×3; c – 18 / 1×1×1.

1– Monte-Carlo procedure, grey gas radiation, K=0.2 m^{-1};

2– Monte-Carlo procedure, non-grey gas radiation (WSGG) $p_{CO_2}+p_{H_2O}$ = 0.22atm, $p_{CO_2} : p_{H_2O}$ = 2.36 :1;

3– Zone method by H. Hottel, data summarized by E. Scholand and taken from [33].

Temperature profile from furnace bottom to exit (upwards see Fig. a) by six vertical layers 1–6 (each of 1 m by height), K: 1 – 1443; 2 – 1485; 3 – 1443; 4 – 1400; 5 – 1364; 6 – 1330.

The single difference between two plants makes the following: the tube wall is erected in the middle plane between refractory walls (cracking furnace) whereas one by another water tube walls arrangement is applied (TVG 8 boiler). The sizes of the cracking furnace section make: 0.33 b×b×2b.

To evaluate the effect of recirculation of combustion products within the boiler space on NO_x formation change of the gases temperature by height was studied.

The results of MC calculations by definition the thermal state of TVG-8 boiler under mixed task statement are presented in Fig. 7 in dependence on recirculation ratio of combustion products.

Divergence of the calculations results makes 0…15% by comparison of our computations by means of MC procedure under WSGG model of gas radiation with that by means E. Scholand's data obtained by means of zone method (Fig. 6).

Grey gases approximation of emissivity increases the difference value till 4…20%.

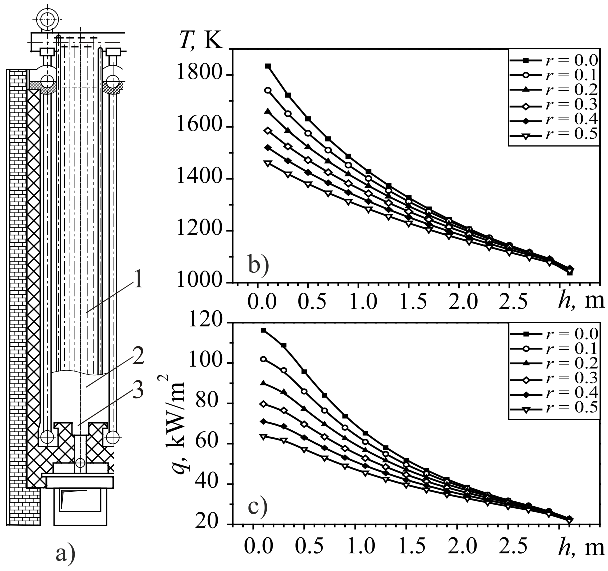

Fig. 7. Profiles of the combustion products temperature T, K (b) and the radiative heat fluxes q, kW/m^2 (c) by height of the boiler TVG-8 furnace (a) in dependence on mass recirculation ratio r. Temperatures, °C: natural gas and combustion air – 25, recirculation gases – 150. Air excess factor λ = 1.2. Natural gas flow rate through section 250 m^3/h.

3.3 Calculation of the reheating furnace (two- and three dimensional temperature pattern within the furnace)

The thermal operation of the continuous furnace have been performed for the pusher type reheating multi-zone furnace of the rolling mill of the "DUNAFERR RT" works (Hungary) (Fig.8). The furnace is arranged with upper and lower zones, the first of them are heated by means of application the roof flat-flame burners, the second – by means of installation the end – face burners.

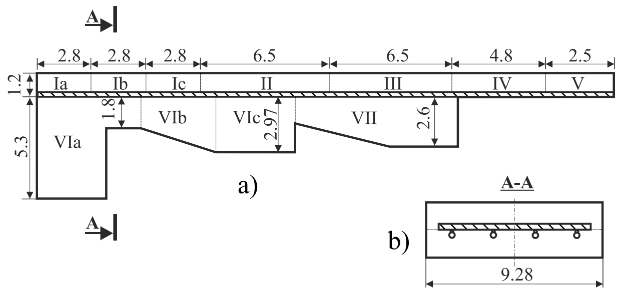

Fig. 8. The "DUNAFERR RT" Company's continuous pusher-type reheating furnace design (layout): a – longitudinal section; b – cross-section. The computation zones numbers are indicated with Roman figures.

The purpose of the computations makes determination of the opportunities to increase the furnace output G_{fur}. The limitation demands make minimal spread (narrow range) of the final reheating temperature for the billets (~1523 K) across the billet (slab) at the furnace exit, approved for use by technology conditions. The slabs are placed across the furnace and are moving by water-cooled skids.

It has been computed the conjugate task of definition the detailed thermal state of the industrial reheating furnace. Both the internal (heat conductivity) and external (radiative exchange) constituents have been solved in 3 – dimensional statement.

By given temperatures of the volume and setting (refractory) zones by means of MC procedures were computed local incident radiative heat fluxes by the billets surface along the furnace length. The last profile forms the boundary conditions by computation the internal task of the billet heating (Fig. 9).

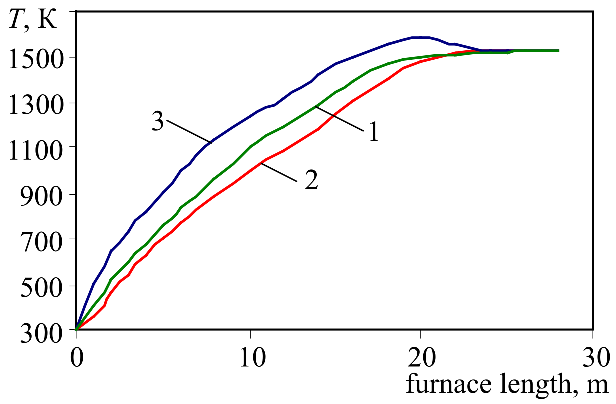

Fig. 9. Thermogram of the billet heating by the furnace length in the central longitudinal plane of the furnace (for middle cross-section by the slab's length).

Steel emissivity factor $\varepsilon_M = 0.9$. Furnace output G_{fur} = 150 t/h. Slab's surfaces computation planes by thickness: 1 – upper; 2 – middle; 3 – lower.

Change of the value and the character of the temperature profiles within the billet of 0.2 m thickness and of 8 m length by change the furnace output G_{fur} has been stated while providing the same profile of the incident radiative heat fluxes by the lower length (Fig. 10).

The following results obtained must be mentioned under condition of increase the furnace output in the range of 130…170 t/h:

- lowering of the final billet reheating temperature (from 1527…1547 K to 1484…1518 K) is accompanied by increase of maximum temperature difference within the billet cross-section;
- overheating of the billet bottom as regards to the upper surface (G_{fur} = 130 t/h) is changed for the higher temperature of the upper surface as regards to lower surface (G_{fur} = 170 t/h) (Fig. 10).

It has been stated that incident heat fluxes profile by the furnace width changes the temperature profile across the billet. Instead of respected overheat of the domains located near the billet end faces (because of the edge effect – three sides heating of the end section) in comparison with the middle section (part) of the billet, we've unexpectedly obtained that the central part of the billets is preheated higher than near the left and right end faces. Such situation is the consequence of reduction of the incident heat fluxes opposite the longitudinal side walls of the furnace.

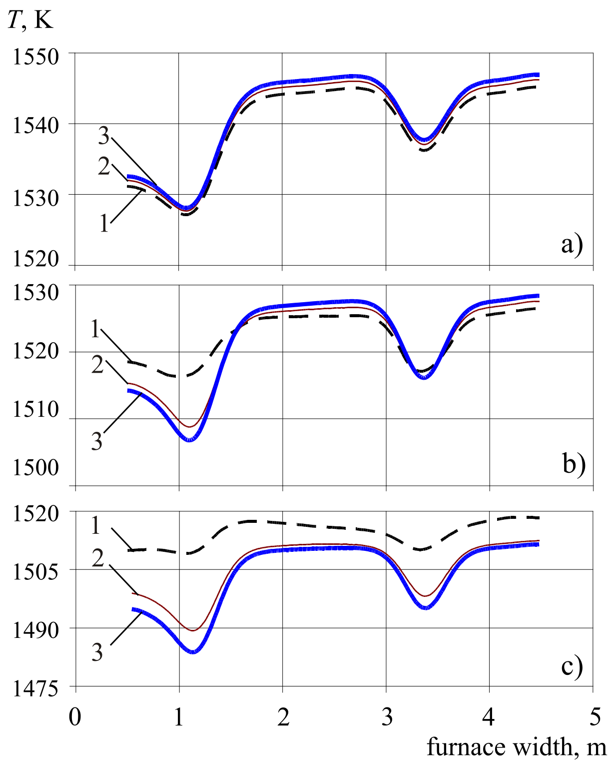

Fig. 10. Temperature profile of the billet across the furnace from the left edge to the axial longitudinal plane, in the exit cross-section plane of the furnace. Furnace output G_{fur}, t/h: a – 130, b – 150, c – 170. Steel emissivity factor $\varepsilon_M = 0.9$. Surfaces computation planes: 1 – upper; 2 – middle; 3 – lower.

4 Application the MC procedures to evaluate the environmental characteristics of combustion process

4.1 Simplified thermodynamic approach

Along with the thermal tasks, the MC technique utilization gives an opportunity of evaluation the harmful substances formation within combustion chambers. The reason is the strong dependence of chemical kinetics (rates of reactions) on local temperature values within the flame – for any polluting component under consideration and of thermodynamically equilibrium concentration – for NO (NO_x) – by peak temperature (like theoretical combustion one or of local maximum value) within the flame and combustion space [34].

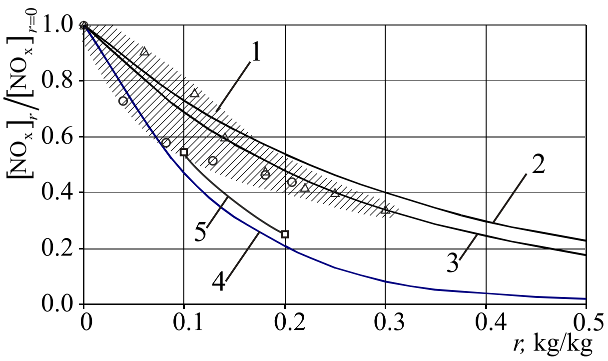

Fig. 11. Dependence of relative reduction of NO_x concentration on mass recirculation ratio *r* of the natural gas/air combustion products.

1 – range of recalculated experimental values for the boilers under consideration in accordance with I. Sigal's data;

○ – boiler TGMP-314A arranged with the modified burners. Temperatures, °C: fuel gas – 20, combustion air – 340, recirculation gases – 350. Air excess factor $\lambda = 1.02 – 1.04$.

Δ – boiler TS-35. Recirculation gases (combustion products) temperature 20°C;

2 – our computation data on characteristic temperatures for TVG-8 boiler: $T_{eff} = T_T - \Delta T_{rad}$.

Temperatures, °C: fuel gas and combustion air – 25, recirculation gases – 150. $\lambda = 1.2$.

3, 4 – our computation data and experimental data by M. Flamme – respectively – for the type 09 burner under natural gas flowrate of 20 m^3/h.

Temperatures, °C: fuel gas – 20, combustion air – 915, recirculation gases – 100. $\lambda = 1.05$.

5 – generalized data [35], cold flue gases recirculation into combustion zone, $\lambda = 1.05$.

The thermodynamical evaluation of NO_x formation by flue gases recirculation within the boilers and furnaces by results of our generalization and in comparison with experimental data is presented in Fig. 11.

The curve 2 (Fig. 11) has been built basing upon redistribution of combustion products temperature by height within furnace space of TVG-8 boiler (see Fig. 7,b) in dependence on flue gases recirculation ratio *r*.

4.2 Application of CFD modeling in combination with MC technique

Monte-Carlo method allows to predict detailed 3D heat fluxes and temperature profiles within HOST Boiler's [36] furnace being divided by more than 2500 volume and surface zones by CFD calculation. These patterns are distinguished by extreme non-uniformity and asymmetric character of gases temperature in accordance with combustion dynamics across the flows and along both stages of reaction, on the one hand, and heat reception depending on arrangement of water-tube screens, on the other hand. Simultaneously heat transfer intensity greatly influences on NO_x formation by combustion due gases temperature distribution.

The 5860 kW commercial Forced Internal Recirculation (FIR) prototype burner was installed and tested by IGT at Detroit Stoker Company (DSC, USA) on watertube boiler, for which a near-term goal of less than 9 vppm NO_x was demonstrated over a 4:1 turndown. This burner has logged > 9,000 hours of commercial operation with no deterioration of commercial performance. Some environmental results of operation are summarized in Table 3.

NO formation prediction by own practice was grounded upon application of global mechanisms for the thermal (Zeldovich-Bowman) and the "prompt" (de Soete) constituents being taken additively; account of the turbulent pulsations of temperature has been performed by introducing of sinusoidal pulsations as PDF (stochastic function).

It has been stated that minimum NO_x yield is provided by FIRB's geometry and operational parameters corresponding to the maximum thermal efficiency of boiler operation.

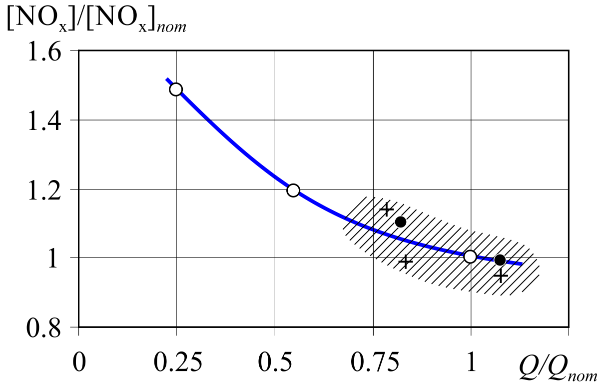

Fig. 12. Dependence of relative NO_x concentration $[NO_x]/[NO_x]_{nom}$ on relative firing rate (load) Q/Q_{nom} of the boiler equipped with FIRB
○ - experimental data; +, • – our predicted data.

Table 3. Environmental characteristic of low-NO_x FIR burner [36].

Characteristic	Operation condition		
	1	2	3
Firing rate, kW	1465	3224	5860
Load, % of Q_{nom}	25	55	100
O_2, %	3.0	2.5	2.8
NO_x, vppm (at 3% O_2)	8.3	6.7	5.6
CO, vppm (at 3% O_2)	40	18	17

In Fig. 12 are compared the results of measurements and calculations on NO_x formation being qualitatively coincided. Unexpected character of $[NO_x]$ change – reduction of NO concentration by thermal load Q (firing rate) increase (Table 3) – has been stated as a result of reduction of residence time within flame zone of high temperature.

5 Conclusion

In spite of the availability of various versions of MC procedure being known for a long period, high demands to computer speed of response reduce possibilities to use MC method. The technique of enhance of computational efficiency of MC procedures has been developed by our team. This method is grounded upon implementation of supplementary conversion of the coordinates, performing in uniform matrix form, finally of four by four matrix size (4×4). By means of mentioned approach we were succeeded in automatic data processing and programming, particularly on assignment of arrangement of the objects under consideration.

The proposed MC procedure is fairly compatible with WSGG model (weighted sum of n grey gases) of account the combustion products selectivity by energy radiation. In framework of this procedure it is assumed that each of the random rays by any direction under consideration is presented by the bundle of n composing beams by all the n radiating quasi-levels of emissivity.

Some designs of boilers of middle capacity have been chosen to predict the peculiarities of heat reception within the tube surfaces. It has been stated that by condition of one – dimensional (by the boiler height) variation of the combustion products or flue gases temperature and by uniform temperature profile within gas medium by the boiler furnace cross section, the absorbed heat fluxes by the furnace perimeter are varied within any horizontal cross-section with deviation of ±25…35% and more. By the boiler height the resulting heat fluxes may varied up to 1.75…3 times.

Industrial furnace modeling demands the solution the conjugate task composed of internal and external constituents. This approach ensures to search for connection of the outer billet reheating conditions: temperature and optic parameters of the furnace working space, non-uniformity of the incident heat fluxes by the billet length (by furnace width) – with the internal characteristics: temperature profile and non - uniformity within the billet.

Due to decrease of the incident heat fluxes in direction from the axial longitudinal plane of the furnace to the side setting walls, the end faces (edges) of the billets are heated weaker and has lower temperature than the central section of the slabs. The lowest temperature level within any billet is related to the locations of contact the slabs with the furnace longitudinal water-cooled guides.

Combined determination of thermal state, power efficiency of the combustion system and environmental consequence of the fuel utilization was realized due application of MC procedure jointly with combustion chemical kinetics or / and thermodynamic equilibrium calculations of NO formation. Each of approaches has been tested successfully for relative NO issues prediction by the boilers operation: in dependence on thermal capacity (computed with account of chemical kinetics) and in conditions of flue gases recirculation estimated by means of approximate thermodynamics technique.

References:

[1] Z. Rudnicki, *Mathematical modeling of Radiative Heat Transfer*, Glivice: Publ. House "Wydawnictwo Politechniki Śląskiej", 2003. – 418p. (in Polish).

[2] B. Soroka, Fuel Furnaces in the problem of enhancement the process of heat- and mass transfer // *In: V Minsk Intern. Heat & Mass transfer Forum Proceedings. – section #9 "Thermophysics and Thermal Engineering of Metallurgical Process"*, 2004. – CD. 9.27 – 35 p. (in Russian).

[3] Bao A., Wang D., Liss W., Using Numerical Simulation Tools to assist the development of a high stability low NO_x industrial burner// *Proceedings of the ASME 2012 Intern. Mechanical Engineering Congress and Exposition IMECE*, 2012, IMECE 2012 – 86300, 9 p.

[4] R. Tucker, J. Rhine, Mathematical modelling of gas – fired furnaces// *In: Industrial and Commercical Gas Utilization*, – CENERTEC. Portugal, 2002, 4p.

[5] P. Lybaert, From CFD to zonal furnace models: an overview of heat treatment furnace modeling//In: *Preprints of the 6th European Conference on Industrial Furnaces and Boilers*, Estoril – Portugal. 2–5 April 2002, pp.1–14.

[6] D.B. Spalding, Mixing and chemical reaction in steady confined turbulent flames// *13th Symposium (Int.) on combustion. Pittsburgh: The Combustion Institute*, 1971, pp.649–657.

[7] H. Ramamurthy, S. Ramadhyany, R. Viskanta, A two – dimensional axisymmetric model for combusting, reacting and radiant flows in radiant tubes, *Journ. of the Inst. of Energy*, Vol.67, September, 1994, pp. 90–100.

[8] L. Lazic, P. Horbaj, Trends in mathematical modelling of gas-fired metallurgical furnaces, *Gas Warme Intern*., H.51, Nr. 6-7, 2002. –S.298–300.

[9] R. Gopinath, V. Ganesan, Numerical predictions of temperature and species concentration in three – dimensional reacting flows – a new approach// *Journ. of the Inst. of Energy*, Vol. 67, March 1994, – pp.10–18.

[10] S. Sampath, V. Ganesan. Numerical prediction of flow and combustion in three-dimensional gas turbine combustors, *Journ. of the Inst. of Energy*, March 1987, pp.15–28.

[11] A. Al Halbouni, A. Scherello, Integration eines Flamelet – Modells in einen CFD – Code zur Berechnung des NO_x – Reducktions potentials durch Reburning, *Gas Warme Intern.*, H.51. Nr.6-7, 2002, pp.288–291.

[12] T.Golec, Numerical calculation of low emission combustion technology// In: *Low-emission combustion Equipment*, Material of conference, 28–30 March, 1996. – Polish Committee on Flame Researches, pp.67–77 (in Polish).

[13] FLUENT 6.3 User's, Chapter 12.3. Radiative Heat Transfer, – 2005.

[14] A. Mazgar, F.B. Nejma, K. Charrada, Numerical analysis of coupled radiation and laminar forced convection in the entrance region of a circular duct for non-grey media: entropy generation. *WSEAS Transactions on Heat and Mass Transfer*, Vol. 3, Issue 3, October 2008, pp.165–176.

[15] K. Domke, Comparison of calculation methods and models in software for computer graphics and radiative heat exchange. *WSEAS Transactions on Heat and Mass Transfer*, Vol. 3, Issue 4, October 2008, pp.198–208.

[16] D.J. Foly, A. van Dam, *Fundamentals of interactive Computer Graphics*, Addison-Wesley Publishing Company, – 1982.

[17] Ju. Tikhomirov, *Programming 3D graphics*, St. Petersburg: BHV – Saint Petersburg, 1998, 256p. (in Russian).

[18] A. Negoitescu, A. Tokar, Opacity Analysis and Estimation of CO_2 Exhausted by a Diesel Engine Vehicle Running under Urban Traffic Conditions. *WSEAS Transactions on Heat and Mass Transfer*, Vol. 7, Issue 2, October 2012, pp.27–36.

[19] P.B. Taylor, P.J. Foster, The total emissivities of luminous and non-luminous flames, *Int. Journ. Heat & Mass Transfer*, Vol.17, No.12, 1974, pp.1591–1605.

[20] J. Strohle, P.J. Coelho, U. Schnell, K.A. Hein, non-grey radiation model for the simulation of coal-fired furnaces // *6th European Conference on Industrial Furnaces and Boilers: Preprints. – Estoril – Portugal. 02-05 (April 2002).* Vol. III: Modelling of Furnaces and Combustion Systems. – 10 pp.

[21] F.R. Steward, P. Cannon, *The calculation of radiative heat flux in a cylindrical furnace using the Monte-Carlo method*, Int. Journal of Heat & Mass Transfer, Vol.14, No.2, 1971, pp.245–261.

[22] H.C. Hottel, A.F.Sarofim, *Radiative transfer*, New York: McGraw – Hill Book Company, 1967, 520 p.

[23] V.P. Barr, Heat transfer model of the tall coke-oven flue, *Iron and Steel Engineer*, January 1987, pp. 57–59.

[24] B. Leckner, Spectral and total emissivity of water vapour and carbon dioxide// *Combustion and Flame*, Vol. 19, 1972, pp.33–48.

[25] A. Soufiani , J.Taine, High temperature gas radiative property parameters of statistical narrow-band model for H_2O, CO_2 and CO, and correlated-K model for H_2O and CO_2 // *Int. J. Heat Mass Transfer*, Vol. 4, 1997, pp. 987–991.

[26] R. Siegel, J.R. Howell, *Thermal radiation heat transfer*, New York: McGraw– Hill Book Company, 1972, 814 p.

[27] B. Soroka, V. Zgurskyy, K. Pyanykh, Development of the Monte-Carlo method to predict radiative heat transfer within the boilers and furnaces // *In: Abstracts of the 13th Intern. Conference on Thermal Engineering and Thermogrammetry (THERMO)*, 18–20 June, 2003, Budapest, Hungary. – Budapest: MATE TE and TGM, 2003, pp.69–78.

[28] B. Soroka, K. Pyanykh, V. Zgursky, M. Khinkis, H. Abbasi, J. Rabovitser, Mathematical modeling of low-emission combustion processes basing upon Monte-Carlo procedures // *Preprints of 5th European conference on industrial furnaces and boilers* (11–14 April 2000), Espinho-Porto (Portugal), Vol. II, 12p.

[29] B. Soroka, K. Pyanykh, V. Zgursky, M. Khinkis, K. Abbassi, I. Rabovitzer, Heat exchange process in low-emission by NO_x boiler furnaces in conditions of two-stage gas burning and of reaction products recirculations// *IV Minsk Intern. Forum "Heat- and Mass transfer MIF-2000" (22-26 May, 2000)*/ Minsk: M. Luikov's Institute of Heat- and Mass Transfer of NASB, Vol.10, 2000, pp.436-445 (in Russian).

[30] V.G. Lisienko, V.V. Volkov, A.L. Goncharov Mathematical modeling of heat exchange within furnaces and assemblies. Kiev: "Naukova dumka" Publ. House. – 1984. – 230 p. (In Russian).

[31] H. Kremer, Möglichkeiten und Grenzen der Strahlungeswarmeubertragung in industriellen Gasfeurungen, *GasWarme Int*, 1994, J.43, H.10. S.482–495.

[32] B.S. Soroka, *Intensification of thermal processes within fuel furnaces*. "Naukova dumka" Publ. House. – 1993. – 416 pp. (In Russian).

[33] E. Scholand, Modern procedures for the calculation of radiant heat transfer in direct-fired tubed furnaces // *Int. Chemical Engineering*, Vol. 23, #4, 1983, pp. 600–610.

[34] B. Soroka, Combined and environmental optimization of fuel-oxidant composition and initial parameters: thermodynamic approach and industrial validation, *Int. Journal of Energy for a Clean Environment*, Vol. 9, Issues 1–3, 2008, pp.65–89.

[35] *Boiler Emission Reference Guide*, 1992, No. 2. – Cleaver-Brooks, 30 p.

[36] B. Soroka, H. Abbasi, J. Rabovitser, Numerical simulation of low-pollutive emission by natural gas combustion // *In: Proceedings of II Intern. conference Industrial Furnaces and Refractory Materials*, 11–13 June 2002, Podbanske-Vysoke Tatry, Slovakia, pp.168–173.